THESIS

ZIKA VIRUS NONCODING SFRNA SEQUESTERS VIRAL RESTRICTION FACTORS INVOLVED IN RNA SPLICING AND NUCLEIC ACID EDITING

Submitted by

Jesús Gustavo Ontiveros Valles

Graduate Degree Program in Cell and Molecular Biology

In partial fulfillment of the requirements

For the Degree of Master of Science

Colorado State University

Fort Collins, Colorado

Spring 2019

Master's Committee:

Advisor: Jeffrey Wilusz

Brian Geiss
Chaoping Chen

ABSTRACT

ZIKA VIRUS NONCODING SFRNA SEQUESTERS VIRAL RESTRICTION FACTORS INVOLVED IN RNA SPLICING AND NUCLEIC ACID EDITING

ZIka virus (ZIKV) is a single-stranded positive sense RNA flavivirus that is transmitted primarily by *Aedes aegypti*. To date, all vector-borne flaviviruses are known to generate stable subgenomic flavivirus RNAs (sfRNA), due to the stalling of the major cytoplasmic 5'-3' exoribonuclease XRN1 at a knot-like three helix junction structure located in viral 3' untranslated regions (UTRs). Formation of sfRNAs not only stalls XRN1, but also represses its function. sfRNA decay intermediates accumulate to high levels in infected cells and studies with other flaviviruses have implicated sfRNAs in cytopathology. Our objective was to characterize the function of ZIKV sfRNAs to gain insight into ZIKV pathogenesis. Specifically, we identified host proteins that interact with ZIKV sfRNA and have begun to evaluate their role in cytopathology and pathogenesis. RNA pull-down experiments revealed that PHAX and SF3B1, critically important RNA splicing factors involved in nuclear-cytoplasmic shuttling, bind sfRNA. Additionally, the cytidine deaminase APOBEC3C was found to bind ZIKV sfRNA. Knockdown and subsequent overexpression of these RNA Binding Proteins (RBPs) identified the nucleic acid deaminase APOBEC3C and the splicing-associated factor PHAX as negative viral restriction factors whose activity may be suppressed and/or altered by sfRNA interaction during ZIKV infection. sfRNA interactions with the splicing factors also resulted in the accumulation of aberrantly spliced transcripts, possibly due to sequestration of the host cell proteins. Thus, in addition to targeting XRN1, sfRNAs appear to interact with a set of RBPs to disrupt cellular mRNA decay regulation as well as other RNA processing events in an effort to compromise multiple steps of RNA metabolism and promote pathogenesis.

ACKNOWLEDGEMENTS

I would like to thank Dr. Jeffrey Wilusz and Dr. Carol Wilusz for allowing me to conduct research in both of their labs, and for the continuous mentorship they have provided over these last few years. I would also like to thank Dr. Joe Russo for continually pushing me to succeed in my scientific endeavors, as he is the reason I can call myself a scientist. Thank you for the kind mentorship and friendship you provided me while I was in the Wilusz^2 lab. I would also like to thank Dr. Dan Michalski for mentorship and advice. A special thank you to Erin Lynch and Cary Mundell for fruitful discussions. Lastly, I would like to thank Phillida, Annie, John and Adam for always taking time out of their days to help me and try to solve any problems I had while conducting my research. Y tambien quiero darle gracias a mis padres, Leticia y Frumencio por siempre apoyándome en todo lo que hecho. Los quiero mucho.

TABLE OF CONTENTS

LIST OF TABLES

LIST OF FIGURES

INTRODUCTION:

The *Flaviviridae* are single-stranded positive-sense RNA viruses which are responsible for an array of human diseases. An estimated 2/3rds of the world's population is at risk for infection by one or more of the 35 flaviviruses which are known to cause disease. Arboviruses are the most recognized members of this virus family and utilize arthropod vectors as an important part of their transmission cycles. These viruses include Dengue virus (DENV), Japanese Encephalitis virus (JEV), Kunjin virus (KUNV), West Nile virus (WNV) and Zika virus (ZIKV). Flavivirus genomic RNA is typically between 10-11kb, and contains a single large polyprotein-encoding open reading frame (ORF) flanked by untranslated regions (UTRs).

A key characteristic common to all arthropod-borne flavivirus infections is the generation and accumulation of a small, single 300-500 base subgenomic flavivirus RNA (sfRNA), which represents the 3' UTR of the viral genomic RNA. sfRNA is not generated using a subgenomic promoter, but rather by stalling of the cellular 5'-3' exoribonuclease XRN1 in its attempts to degrade viral, positive-sense transcripts within infected cells (Funk et al. 2010; Silva et al. 2010; Chapman et al. 2014a; Chapman et al. 2014b). All arthropod-borne flaviviruses tested to date contain a three-helix junction knot-like structure in the proximal portion of their 3' UTR that stalls XRN1 (Slonchak and Khromykh 2018). Interestingly, sfRNA generation results in repression of XRN1 activity in DENV and KUNV infection, presumably due to slow release of XRN1 from the knot-like RNA structure (Moon et al., 2012; 2015). sfRNA-mediated XRN1 repression also appears to feedback in some fashion and shut down upstream functions of the decay pathway (Moon et al. 2012; Moon and Wilusz 2013; Steckelberg et al. 2018), where dysregulated gene expression results in stabilization of cellular mRNAs. This effect can be particularly dramatic for short-lived mRNAs, such as cytokines and immune factors (Moon et al. 2012; Moon et al., 2015). The

abundant sfRNA in the cell can also serve as a sponge on which cellular RNA binding proteins can be sequestered, resulting in functional repression of a variety of RNA Binding Proteins (RBPs). To date, several cellular pathways that are targeted by sfRNA have been identified including innate immunity, interferon and RNA interference (Moon et al. 2015; Barnhart et al. 2013; Bidet et al. 2014; Bidet et al., 2017; Funk et al., 2010; Hu et al., 2017).

ZIKV is a flavivirus which was discovered in 1947 in the forests of Uganda, and is transmitted by *Aedes aegypti*. The majority of ZIKV infections are asymptomatic, while those who do display symptoms typically have rash, mild fever, arthralgia and conjunctivitis (Hu et al., 2017; Petrova et al., 2019; Weger-Lucarelli et al., 2017). In some instances, adults can even develop Guillain-Barre syndrome where the immune system mistakenly damages neuronal cells and can cause debilitating movement (Hu et al., 2017). Notably, ZIKV infection during pregnancy can result in microcephaly, brain/eye abnormalities and even fetal loss due to the wide range of neurological damage that ZIKV causes (Hu et al., 2017; Weger-Lucarelli et al., 2017). Flaviviral-associated pathogenesis mechanisms still largely remain unclear, and thus it is important to understand how these viruses interface with host-cell factors.

Gene expression regulation through post-transcriptional mechanisms is a complex cellular process which is critically important for maintaining cellular homeostasis. Therefore it is not surprising that many aspects of post-transcriptional control are targeted and disrupted by RNA viruses during infection (Moon et al., 2012; Petrova et al., 2019). For instance, RNA splicing is a highly regulated post-transcriptional process that relies on the proper localization of the macromolecular complex known as the spliceosome in order to avoid aberrant splicing events within the cell (Wu et al., 2018). Mutations in the splicing factors SF3B1, a component of the U2 snRNP, can induce alternative splice sites in a subset of targeted host cell genes (Darman et al. 2015; Wu et al 2018). Recent transcriptome analysis of ZIKV-

infected human neural progenitor cells identified hundreds of instances where aberrant alternative splicing occurred in more than 200 different RNAs (Hu et al., 2017b). Precisely how a cytoplasmic virus such as ZIKV induces significant mis-splicing within infected cells remains unclear – and providing insight into these mechanisms was one of the goals of this thesis.

Likewise, other aspects of post-transcriptional control can be impacted by RNA virus infections. The cellular mRNA decay machinery, a fundamental regulator of both quantity and quality of gene expression (Schoenberg and Maquat 2012), can also be targeted (Schoenberg et al., 2012). mRNA decay begins with deadenylation of the transcript, followed by the decapping of the 7-methylguanosine cap (Schoenberg et al., 2012). The monophosphorylated transcript is then reduced to single nucleotides via the action of the highly processive cytoplasmic 5'-3' exoribonuclease XRN1 (Schoenberg et al., 2012). Evidence has mounted revealing that transcripts of RNA viruses are also actively targeted by the cellular RNA decay machinery (Moon and Wilusz 2013). Thus, any alteration in the cell's ability to regulate RNA decay can have dramatic effects on the outcome and pathogenesis associated with viral infection.

Finally, RNA editing can also have an impact on viral infections, as it can greatly expand the coding capacity of the transcriptome (Kung et al., 2018). The process consists of the deamination of adenosine to inosine (decoded as guanosine) or a cytosine to uracil and is catalyzed by one of two classes of deaminases: ADAR family enzymes that catalyze A to I (read as G) editing, and AID/APOBEC family of enzymes that catalyze C to U (Lerner et al. 2018). RNA editing activity has been reported in APOBEC1, APOBEC3A (Sharma et al. 2015), and APOBEC3G (Sharma et al. 2016), but not for other members of the family to date. APOBEC3G has been implicated as a major restriction factor for retroviruses (Zhu et al., 2015). There is also some evidence that APOBEC3H has antiviral functions against hepatitis C virus (HCV), a member of the *Flaviviridae* family of viruses (Peng et al., 2011).

The purpose of this study was to catalogue major RNA binding proteins which interact with sfRNA generated during ZIKV infection and provide foundational data for potential molecular mechanisms of sfRNA-associated pathology. In this study we demonstrate that ZIKV infection in human cells leads to the accumulation of sfRNA which selectively associates with over 20 RNA binding proteins which affect a wide range of post-transcriptional cellular processes. We discovered that sfRNA associated with host cell splicing factors PHAX and SF3B1, as well as the cytidine deaminase APOBEC3C. Interestingly, SF3B1-mediated RNA splicing was shown to be significantly dysregulated during ZIKV infection leading to the production of novel, aberrantly spliced transcripts. Thus, generation of sfRNA during ZIKV infection appears to not only stall and subsequently repress the function of the 5'-3' cellular exoribonuclease XRN1, but also appears to act as a protein sponge for a multitude of host RNA binding proteins. By disrupting aspects of cellular gene expression, ZIKV infection hinders the cell's ability to effectively respond to viral infection by sequestering viral restriction factors.

MATERIALS AND METHODS:

PCR/cloning/plasmid generation:

Cloning for FLAG-tagged protein over-expression:

The p3XFLAG-CMV™- 10 Expression Vector (Sigma-Aldrich: #E7658) was used for generating 3x N-terminal FLAG-tagged proteins transfected into HEK293T cells. cDNA from HEK293T cells was used as template for the PCR-based amplification of select genes using sequence-specific primers engineered with restriction sites at their 5' & 3' ends to allow for ligation into the polylinker region of p3XFLAG-CMV™-10 Expression Vector (See Table 1 for a detailed list of all primer sequences used in this study).

Table 1: N Terminal 3x-FLAG Tag Cloning Primers

Primer	Sequence (5'-3')
APOBEC3C EcoR1 - Forward	GATCGAATTCAAATCCACAGATCAGAAACCC
APOBEC3C BamH1 - Reverse	TCGCGGATCCTCACTGGAGACTCTCCCGTA
PHAX EcoR1 - Forward	GATCGAATTCAGCGTTGGAGGTCGGCGATATG
PHAX BamH1 - Reverse	TCGCGGATCCTTAAAAGATCTCCAAATCAT

Cloning and sequence analysis of alternatively spliced products:

cDNA from mock-infected (control) or ZIKV-infected (48 hours post infection) HEK293T cells was used as template for the PCR-based amplification of the human SRSF7 gene region spanning exons 2-8

using the following specific primers: SRSF7 Exon 2 Forward: 5'-GAA CTA TCG ACA GGC ATG CC-3'; SRSF7 Exon 8 Reverse: 5'- CTT CTG CGA GGA CTT CCT GAT-3'. PCR products were separated via agarose gel electrophoresis. Novel PCR products of interest were excised from the gel, purified using the Wizard SV Gel and PCR extraction kit (Promega-Ref#A9281), and sequenced via Sanger sequencing. Sequencing reads were aligned using Serial Cloner software (version 2.6.1).

Table 2: SRSF7 Splice Check Primers

Primer	Sequence
SRSF7 Sequencing Reverse	CTTCTGCGAGGACTTCCTGAT
SRSF7 Amplicon Forward	TGCAGTACGAGGACTGGATG

Cell lines and virus propagation:

Human embryonic kidney 293T (HEK293T) and African green monkey (*Cercopithecus aethiops*) kidney cells (Vero) were maintained in Dulbecco's Modified Eagle's medium (DMEM; Mediatech-Corning) supplemented with 10% newborn calf serum (NBCF; Peak Serums), 1% streptomycin/penicillin (Fisher Scientific-Hyclone), 0.5% L-glutamine (Fisher Scientific-Hyclone) and incubated at 37°C in the presence of 5% CO^2. Human choriocarcinoma (JAR) cells were maintained in RPMI1640 1x with L-glutamine (Corning: Ref 10-040-CV) supplemented with 10% newborn calf serum (NBFC; Peak Serums), 1% streptomycin/penicillin (Fisher Scientific-Hyclone), and 0.5% L-glutamine (Fisher Scientific-Hyclone), and incubated at 37°C in the presence of 5% CO^2. HEK293T, Vero, and JAR cells were routinely passaged (every 72-96 hours) by washing the monolayer with cold 1X-phosphate buffered saline (PBS; Corning) followed by incubation at 37°C with a 0.25% trypsin solution (Fisher Scientific-Hyclone) until the cells

detached. Cells and buffer were then diluted 1:1 with fresh media, transferred to a 15mL conical tube and centrifuged at 500xg for five minutes. The cell pellet was resuspended in fresh media by pipetting and routinely passaged at a 1:10 dilution.

RNA pull-downs of associated protein factors:

1ug of each *in vitro* transcribed, biotinylated ZIKV 3' UTR, DENV-2 3' UTR and pGEM-sequence derived (control) RNA was used as starting material for the RNA pull-down. 100uL of uMacs Streptavidin magnetic beads (Miltenyi Biotech) was added to each of the biotinylated RNA preparations, and tubes were incubated at room temperature on a table-top rocker for 10min to allow biotinylated-RNAs to bind the streptavidin magnetic beads. Next, 350uL of pre-cleared HeLa cell cytoplasmic extract supplemented with 5ul protease inhibitor cocktail (Sigma-Aldrich) was added to each reaction tube and incubated at 4°C with rotation for 60min. uMacs magnetic bead columns (Miltenyi Biotech) were set-up in the supplied magnetic stand and equilibrated with 100uL of Protein Equilibration buffer (Miltenyi Biotech). The columns were rinsed 2X with 200uL Binding/Wash Buffer (10mM HEPES pH 7.0, 200mM KCL, 10% glycerol, 1mM EDTA, 1mM DTT, 0.5% Triton X-100, Ribolock RNase Inhibitor [1 U/µL] (Thermo Scientific). Reaction mixtures were then applied to the center of the equilibrated and washed column, and the flow-through collected in a separate 1.5mL microfuge tube. Columns were washed 4X with 1mL Binding/Wash buffer (Miltenyi Biotech). RNA-binding proteins (RBPs) were eluted from the RNAs via the addition of Binding/Wash buffer supplemented with 1M NaCl and collected in 1.5mL microfuge tubes. A 10% SDS-PAGE gel was cast and run in a laminar flow hood to minimize contamination with external protein sources. Equal volumes of eluted RBPs plus 2X-SDS protein load dye (100 mM Tris-Cl (pH 6.8) 4% (w/v) SDS, 0.2% (w/v) bromophenol blue, 20% (v/v) glycerol), 200 mM dithiothreitol (DTT)), were mixed, boiled for 5min, and loaded into separate wells. Protein samples were run through the stack and just into the resolving gel before being Coomassie stained and visualized with destain (40% methanol, 10%

glacial acetic acid solution) solution. Protein bands were excised from the gel, placed in a 1.5mL microfuge tube with 500uL destain and submitted to the Proteomics and Metabolomics Facility at Colorado State University for trypsin digestion and LC-MS/MS protein identification.

Western Blotting:

Sample cells were collected in 15mL conical tubes, spun at 500xg for 5min to pellet cells, and washed 2x with 10ml ice cold PBS. Washed cell pellets were resuspended in 1ml low-stringency RIPA buffer (50mM Tris - HCl pH7.5, 1% NP40, 0.5% sodium deoxycholate, 0.05% SDS, 1mM EDTA, 150mM NaCl) supplemented with 0.2mM PMSF and protease inhibitor cocktail (Sigma-Aldrich # P8340-5ML), transferred to a 1.5mL microfuge tube and incubated at 4°C with rotation for 10min. Lysate was transferred to a 1.5mL microfuge tube, filtered through a 25-gauge needle to shear the chromatin, spun to pellet debris, and finally transferred to a new 1.5mL microfuge tube. Equal volume of lysate and 2X-SDS load dye were mixed, boiled for 5 minutes and loaded onto a 10% SDS-PAGE gel. Proteins were transferred to PVDF membrane (Immobilon-P; Ref: IPVH00010) using a semi-dry electrophoretic transfer cell (Bio-Rad; Cat#1703940). Transferred blots were blocked in Blocking buffer (1X PBS-Tween 20 solution supplemented with 5% powdered milk) for 60min at room temperature with rotation. Probing blots (see table 3 for details on antibodies): 5mL fresh blocking buffer + primary antibody was rotated with the blots for 60min at room temperature, then washed 3X 10min each with 1X PBS-Tween 20 solution. 5mL fresh blocking buffer and secondary antibody was rotated with the blots for 60min at room temperature, washed 3X 10min each with 1X PBS-Tween 20 solution, then developed with SuperSignal West Dura extended duration substrate (Thermo Scientific-Ref:34075). Blots were imaged using the Azure Sapphire Biomolecular Imager (Azure Biosystems).

In-vivo formaldehyde crosslinking and RNA co-immunoprecipitation and analysis:

10cm dishes of ZIKV-infected (48 hpi) HEK293T cells were scraped from the dish and collected in 15mL conical tubes. Cells were washed once with complete media, 2X with 5mL ice-cold 1xPBS, and resuspended in 10mL 1xPBS. Formaldehyde (0.3% final concentration) was added to the tubes and incubated at room temperature with gentle rocking for 10min. 1.4mL of 2M glycine pH 7.0 was added and incubation continued for an additional five minutes. Cells were washed 2X with 5mL ice cold PBS, then whole cell lysate generated (see section on Western Blotting for detailed lysate prep). Lysate was pre-cleared by incubating with 20uL packed Protein A magnetic beads (NEB - #S1425S) for 1 hour at 4°C. Beads were separated from cleared supernatant using a magnetic separation rack (NEB#S1506S), and a portion of the lysate was set aside as "Input". The remaining lysate was divided equally between two 1.5mL E. tubes, and each tube of lysate diluted with 250uL low-stringency RIPA buffer + 10uL corresponding primary antibody in one tube and 10uL normal-rabbit IgG in the control tube (Santa Cruz Biotech-SC-2025). Tubes rotated with primary antibody for 1 hour at 4°C, then 20uL Protein A magnetic beads were added to each tube and the tubes incubated at 4°C for an additional hour.

Table 3: Antibodies

Protein Target	Antibody	Dilution Used (Western Blot)
APOBEC3C	APOBEC3C antibody (cat.#GTX102164) - GeneTex	1:500
PHAX	Anti-PHAX (ab157096) - Abcam	1:1000
SF3B1	Anti-SAP155 antibody (ab66774) - Abcam	1:1000
GAPDH	Anti-GAPDH, clone 6C5 – Millipore Sigma	1:1000

FLAG-tag	Monoclonal ANTI-FLAG® M2– Millipore Sigma (F1804-200UG)	1:1000
Anti-Mouse 2^{o}Ab	Goat anti-mouse IgG-HRP (sc2005) – Santa Cruz Biotech	1:2500
Anti-Rabbit 2^{o}Ab	Goat anti-Rabbit IgG-HRP (sc2030) – Santa Cruz Biotech	1:2500

Bead Washes:

Tubes were placed in the magnetic separation rack, supernatant removed and discarded, and beads washed 5x with 1mL high-stringency RIPA buffer (base recipe: 50mM Tris – HCl pH 7.5, 1% NP-40, 1% sodium deoxycholate, 0.1% SDS, 1mM EDTA, 1M NaCl, 1M Urea) supplemented with 1mM PMSF and protease inhibitor cocktail (Sigma-Aldrich # P8340-5ML). Beads were resuspended in 100uL TEBS buffer, incubated at 70˚C for 45min to reverse crosslinking, and 300uL TRIzol (Invitrogen) added to each 100uL sample (in TEDS buffer). RNA extraction was done via the addition of 80uL chloroform to the TRIzol reagent, following the manufacturer's procedure. Reverse transcription was done using 1ug total RNA as described above. The abundance of GAPDH and ZIKV RNA was determined by quantitative digital droplet PCR using Bio-Rad's QX200 Droplet Digital PCR System and QX200 EvaGreen ddPCR Supermix (Bio-Rad) for each primary antibody use to immunoprecipitated the targeted protein. The primers used were as follows: GAPDH forward: 5'-TCTT TTGCGTCGCCAGCCGA; GAPDH reverse: 5'-ACCAGGCGC CCAATACGACC; ZIKV RNA Forward: 5'-AGGATCATAGGTGATGAAGAAAAGT, ZIKV RNA Reverse: 5'-GCACCAATCTTAATGTTGTCAGG. QuantSoft software generates the absolute copy number of the target DNA molecule in copies/uL. First the data was normalized to GAPDH across all samples. Next, fold changes in the target gene were calculated comparing experimental samples to control treated samples.

The data shown represent the mean values from three independent experiments. P-values were determined by a Student's t-test.

Mass spectrometry:

LC-MS/MS protein identification was performed by the Proteomics and Metabolomics Facility at Colorado State University. Scaffold 4 software was used to analyze the mass spectrometry data.

siRNA knockdown in ZIKV-infected HEK293T Cells:

10cm plates were seeded with HEK293T cells so that the plates were ~30% confluent at the time the experiment began. Day 1(1st siRNA hit): control siRNA or siRNAs-targeting specific cellular proteins were transfected into HEK293T cells using JetPrime transfection reagent (Polyplus) according to the manufacturer's instructions, then returned to the 37°C incubator for 24 hours. Day 2 (2nd siRNA hit): same procedure as Day 1. Day 3 (ZIKV infection + 3rd siRNA hit): decant and discard the HEK293T growth media and replace half the original volume with fresh HEK293T media. Infect cells by adding freshly thawed Zika virus (Multiplicity of Infection (MOI) of ~10) to the dish, gently rocking to evenly distribute the virus across the cellular monolayer and incubating at 37°C for 60min. Viral media was then decanted and discarded, cells were rinsed once with 5ml 1X PBS to remove any virus particles not taken up by the cells, and 10mL fresh HEK293T media added back to the cells. Cells were allowed to recover from the infection by incubating at 37°C for 1 hour. Following the 1 hour recovery period, plates were subjected to their 3rd siRNA transfection (same procedure as described for Day 1), then returned to the 37°C incubator for 48 hours. Day 5 (collecting cellular supernatant and harvesting cells): The media from each ZIKV-infected cell plate was collected in a 15mL conical tube, spun at 500xg for 5min to pellet any debris, and aliquoted into 1.5mL microfuge tubes in 1mL aliquots for use with focus forming assays. Cells were

harvested with TRIzol reagent (Invitrogen), adding 4mL to each 10cm plate, incubating at room temperature for 5min with gentle rocking and collecting in 1.5mL microfuge tubes in 1mL aliquots.

Total RNA was isolated from the TRIzol reagent following the manufacturer's protocol and treated with DNase I (Fermentas). Reverse transcription was done using 1 ug of total RNA with Improm-II Reverse Transcriptase (Promega) and random hexamer primers to generate cDNA. The abundance levels of GAPDH mRNA, mRNAs targeted via the siRNAs for knockdown, and ZIKV RNA were determined by quantitative digital droplet PCR using the Bio-Rad QX200 Droplet Digital PCR System and QX200 EvaGreen ddPCR Supermix. The primers used were as follows: GAPDH forward: 5'-TCTT TTGCGTCGCCAGCCGA; GAPDH reverse: 5'-ACCAGGCGC CCAATACGACC; ZIKV RNA Forward: 5'-AGGATCATAGGTGATGAAGAAAAGT; ZIKV RNA Reverse: 5'- GCACCAATCTTAATGTTGTCAGG. The QuantSoft software (Bio-Rad) generates the absolute copy number of the target DNA molecule in copies/uL. First the data was normalized to GAPDH across all samples. Next, fold changes in the target gene were calculated comparing experimental samples to control treated samples. The data shown represent the mean values from three independent experiments. P-values were determined by a Student's t-test. Total Protein (from the same sample) was isolated from the TRIzol reagent following the manufacturer's protocol. Protein pellets were resuspended in a 3:1 mixture of 8M urea : 1% SDS. Protein concentrations were determined using the Qubit 3.0 Fluorometer (Thermo Fisher) and accompanying Qubit Protein Assay Kit (Thermo Fisher). Equal weight of protein from each sample was then separated based on size via SDS-PAGE. Proteins were transferred to PVDF-membranes (Immobilon-P; Ref: IPVH00010) using a semi-dry electrophoretic transfer cell (Bio-Rad; Cat#1703940). Transferred blots were blocked in blocking buffer (1X PBS-Tween 20 solution supplemented with 5% powdered milk) for 60min at room temperature with rotation. Probing blots (see table 3 for details on antibodies): 5mL fresh blocking buffer + primary antibody was rotated with the blots for 60min at room temperature or overnight at 4°C, then washed 3X 10min each with 1X PBS-Tween 20 solution. 5mL fresh blocking buffer

+ secondary antibody were rotated with the blots for 60min at room temperature, washed 3X 10 minute each with 1X PBS-Tween 20 solution, then developed with SuperSignal West Dura extended duration substrate (Thermo Scientific-Ref:34075). Blots were imaged using the Azure Sapphire Biomolecular Imager (Azure Biosystems).

Table 4: siRNA Sequences

siRNAs	Sequence (5'-3')
APOBEC3C	GAAACCAGGTGGATTCTGA
PHAX 1	GUAUCAGCGAGGAACAAAUUA
PHAX 2	GAGUAUAUAGCACAGGAUUUA
SF3B1	CGAGUUUGCUUGGUCAGAA
Control	SIC001-1NMOL

Protein overexpression in ZIKV-infected HEK293T cells:

10cm plates were seeded with HEK293T cells so that the plates were ~30% confluent at the time the experiment began. Day 1 (1st DNA transfection): p3XFLAG-CMV™-10 Expression Vectors (Sigma-Aldrich: #E7658) harboring one of the three identified mammalian protein gene sequences or no inserted sequence (Empty-Vector) were transfected into Hek293T cells using jetPrime transfection reagent (Polyplus) according to the manufacturer's instructions, then returned to the 37°C incubator for 24 hours. Day 2 (2nd DNA transfection): same procedure as Day 1. Day 3 (ZIKV infection + 3rd DNA transfection): decant and discard the HEK293T growth media and replace half the original volume with fresh HEK293T media. Cells were infected by adding freshly thawed Zika virus (MOI of ~10) to the dish,

gently rocking the evenly distribute the virus across the cellular monolayer and incubating at 37°C for 60min. Viral media was then decanted and discarded, cells were rinsed once with 5ml 1X PBS to remove any virus particles not taken up by the cells, and 10mL fresh HEK293T media added back to the cells. Cells were allowed to recover from the infection by incubating at 37°C for 1 hour. Following the 1 hour recovery period, plates were subjected to their 3rd DNA transfection (same procedure as described for Day 1), then returned to the 37°C incubator for 48 hours. Day 5 (collecting cellular supernatant and harvesting cells): The media from each ZIKV-infected cell plate was collected in a 15mL conical tube, spun at 500xg for 5min to pellet any debris, and aliquoted into 1.5mL microfuge tubes in 1mL aliquots for use in focus forming assays. Cells were harvested with TRIzol reagent (Invitrogen), adding 4mL to each 10cm plate, incubating at room temperature for 5 minutes with gentle rocking and collecting in 1.5mL microfuge tubes in 1mL aliquots. Total RNA and Total Protein was isolated from each TRIzol sample as described in the siRNA knockdown in ZIKV infected HEK293T cells above.

Virus Preparation:

All ZIKV infections were performed using ZIKV strain PRVABC59. Infectious Zika virus particles were obtained from infectious cDNA clones, described in detail in (Weger- Lucarelli al., 2017). Propagation of the virus was conducted in Vero cells as follows: 15cm dishes were seeded with enough Vero cells in cDMEM supplemented with 10% FBS and 12.5mM HEPES so that plates were ~70% confluent 24hr later. The next day media was removed from the plates and replaced with half the original volume of cDMEM supplemented with 2% FBS and 12.5mM HEPES. Zika virus (MOI of ~0.1) was added to the media and rocked gently to evenly distribute the virus, then incubated at 37^{o}C for 60min. The remaining volume of media (cDMEM supplemented with 2% FBS and 12.5mM HEPES) was then added back to the cells and plates were incubated at 37^{o}C for ~72 hours. When ~50% of the cells were dead, media was collected in 15mL conical tubes, spun at 500xg for 5 minutes to pellet any cellular

debris, and aliquoted virus-containing media into 1mL aliquots and frozen at -80°C. Newly propagated Zika virus stocks were titered via focus forming assays as described in (Weger-Lucarelli et al., 2017).

Table 5: ddPCR Primers

Primer Targets	Forward Primer (5'-3')	Reverse Primer (5'-3')
APOBEC3C	GTGGGACAGGGACAAGCATA	CCCGTCTTCCAGGAGACAAC
PHAX	ACAGGCTAGGGAACAGACCA	TCACTACTCGGGCTATCAGGT
SF3B1	CCCAGAGCGTCTTGATCCTT	AGCTTTTTCTCGTAGCTGTTGC
GAPDH	TCTTTTGCGTCGCCAGCCGA	ACCAGGCGCCCAATACGACC
EDC3	ATTTCTCTCACCCGGCCTTTCC	CGTAATGTCACCTGCCCTGAAG
ZIKV 3' UTR	CATGAGTTTCCACCACGCTG	AGACCCATGGATTTCCCCAC
ZIKV Genomic RNA	AGGATCATAGGTGATGAAGAAAAGT	GCACCAATCTTAATGTTGTCAGG

RESULTS:

ZIKV and DENV bind cellular RNA binding proteins involved in a multitude of post-transcriptional processes

A substantial amount of sfRNA in infected cells is generated as xrRNA structures in flavivirus genomic plus sense RNAs stall and repress XRN1 activity (Moon et al., 2012; Pijlman et al., 2008; Silva et al., 2010; Chapman et al., 2014). The extensive accumulation of these sfRNAs may also serve as a sponge to sequester cellular RNA binding proteins and influence host-virus interactions that subsequently impact cellular physiology. In fact, flavivirus sfRNAs have previously demonstrated the capacity to interact with proteins involved in interferon responses, translational regulation, RNAi and innate immunity (Moon et al., 2015; Lerner et al., 2018; Sharma et al., 2015; Sharma et al., 2016; Petrova et al., 2019). Thus we hypothesized that sfRNA may bind to a series of RNA binding proteins and may have a broader impact on the RNA biology of the host cell than previously anticipated. To further elaborate the role of sfRNA and test this hypothesis, biotinylated RNA pulldown assays were performed in collaboration with Dr. Dan Michalski in the lab using ZIKV sfRNA, DENV sfRNA or control RNA and HeLa cytoplasmic extracts. In order to promote the identification of biologically relevant, high affinity interactions in this experiment, we instituted two requirements. First, the pull down assays were performed under relatively stringent conditions using high (300mM) salt concentrations to enrich for interactions with higher stability. Second, following protein identification by mass spectrometry, we only chose to pursue proteins that interacted with both DENV-2 and ZIKV sfRNA but not with the control transcript. This selection should bias our future analyses towards proteins that had a general effect on flavivirus biology. Using these criteria, 28 proteins were found to be associated with both ZIKV and DENV sfRNA, and 21 of the proteins identified were associated with RNA biological processes including

RNA decay, translation, splicing and editing (Fig. 1A and B). These 21 proteins therefore became the focal point of subsequent analyses.

A

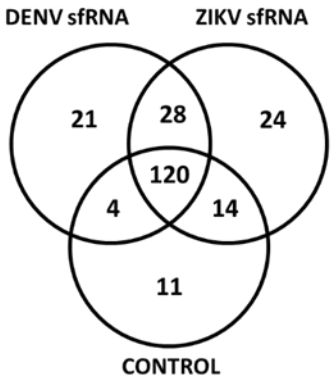

B

BIOLOGICAL PROCESS:	sfRNA-BINDING PROTEINS:
RNA Decay	DDX6, EDC3
RNA Splicing	PHAX, SF3B1, SF3B2,PRPF19, PPIH, NMP1, PCBP2, RTCB, HNRNPK, HNRNPF, HNRNPH1
Nucleic Acid Editing	APOBEC3C
Translation/Ribosome Factors	LSM14B, RPL22, RPL17, RPL7a, EEF1A1, TDRD3, BRIX1

C

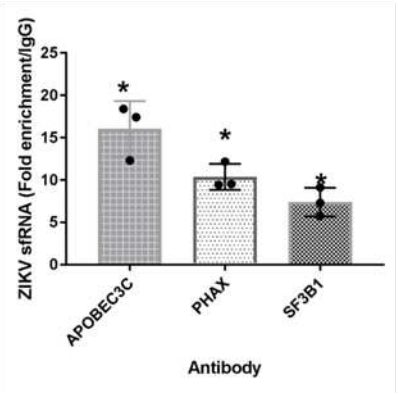

Figure 1: ZIKV and DENV-2 sfRNAs interact with a common set of 28 proteins that impact a variety of aspects of cellular post-transcriptional gene regulation.
Biotinylated RNAs containing the DENV-2 3' UTR, ZIKV sfRNA or a size-matched control transcript were incubated with HeLa cytoplasmic extracts. Proteins that co-purified with the RNAs on streptavidin beads were identified by mass spectrometry. Panel A: a Venn diagram depicting the number and commonality of human host-cell RNA-binding proteins identified via mass spectrometry for each RNA. Panel B shows the relationship of proteins that bound to both the ZIKV and DENV sfRNA to associated post-transcriptional processes. Panel C: ZIKV sfRNA directly binds to a variety of cellular RNA-binding proteins in infected cells. 293T cells were infected with ZIKV for 48 hrs. Formaldehyde was added to the cultures to stabilize RNA-protein complexes and total cell extracts were prepared. Antibodies to the cytidine deaminase APOBEC3C, RNA splicing factors PHAX and SF3B1, or normal rabbit IgG were added to the extracts to immunoprecipitate RNA-protein complexes. Co-purifying RNAs were analyzed by digital droplet RT-PCR using primers to the Zika virus sfRNA/3'-UTR. The abundance of ZIKV RNA co-precipitated using the various antibodies was determined relative to the amount pulled down in the normal rabbit IgG control. Results are shown as the average +/- standard deviation from three independent infections.

I chose to focus my efforts in the areas of RNA splicing and editing. Three representative proteins, APOBEC3C, PHAX and SF3B1, involved in RNA splicing and nucleic acid editing were validated as bona fide sfRNA interactions proteins by performing RNA co-immunoprecipitation experiments using protein specific antibodies and ZIKV infected cell extracts. As seen in Fig. 1C, antibodies to all 3 proteins co-precipitated ZIKV sfRNA significantly (7-15 fold) above the IgG control background. Therefore we conclude that both ZIKV and DENV sfRNA interact with these three proteins in a specific manner during infection and may sequester them, thus resulting in dysregulation of their associated post-transcriptional processes.

ZIKV sfRNA sequesters negative restriction factors involved in nucleic acid editing and RNA splicing

We focused on determining the effect of these three proteins, one nucleic acid deaminase and two of which are involved in RNA splicing, on ZIKV infection dynamics. APOBEC3C is a cytidine deaminase localized to both the nucleus and cytoplasm and has been implicated in deamination of C to T residues in single stranded DNA (Timilsina et al., 2018). A close relative of this protein has been implicated in post-transcriptional editing of C residues to U in RNA. PHAX is involved in U snRNA nuclear export for maturation in the cytoplasm (Mourao et al., 2010). SF3B1is part of the U2 snRNP complex, a core component of the cellular splicing machinery. siRNA mediated knockdown of each of the three proteins was performed and significant reductions in levels of both mRNA and protein levels were observed (Fig. 2). SF3B1 knockdown unfortunately resulted in cells with poor growth characteristics and this factor was thus excluded from further analyses. As seen in Fig. 3A, APOBEC3C and PHAX knockdown resulted in a significant ~4X increase in ZIKV viral RNA in infected cells. To complement these results, focus forming assays were performed to observe the amount of mature/infectious virus actively being released by cells. As seen in Fig. 3B, a significant increase in viral titers was observed. Conversely, 2-fold

overexpression of these two proteins resulted in a significant decrease in ZIKV viral RNA alongside a significant reduction in viral titers. Thus we conclude that the nucleic acid deaminase APOBEC3C and the RNA splicing-associated factor PHAX are negative viral restriction factors for a ZIKV infection. As discussed further below, we hypothesize that their activity may naturally be at least partially suppressed and/or altered by sfRNA interaction during ZIKV infection.

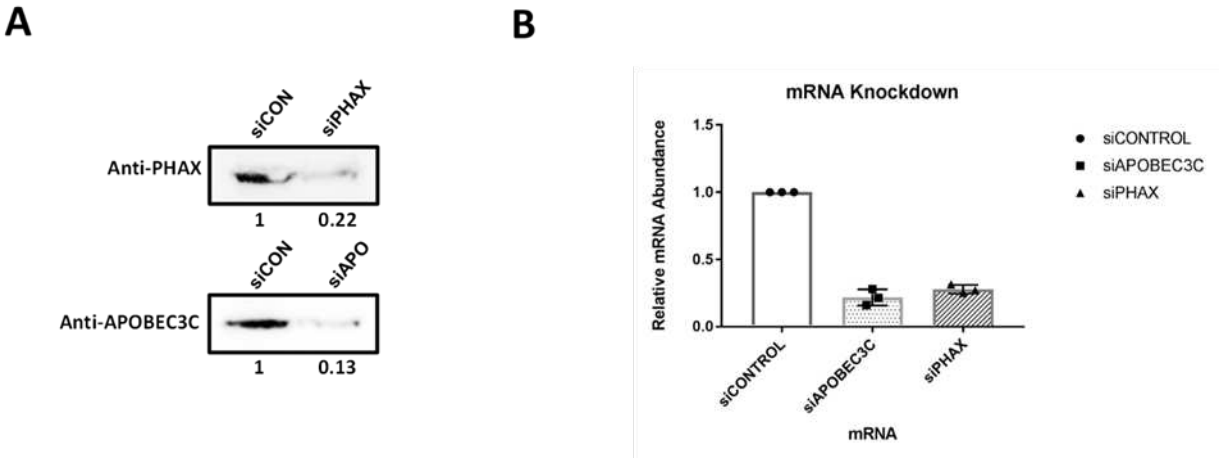

Figure 2: siRNA mediated knockdown of the cytidine deaminase APOBEC3C and the RNA splicing factor PHAX

Panel A: Representative western blot depicting endogenous APOBEC3C and PHAX protein levels in ZIK-infected HEK 293T cells treated with either a control siRNA (siCON lanes), or an siRNA targeting APOBEC3C (siAPO lane) or a siRNA targeting PHAX (siPHAX lane). Band intensity was quantified using ImageJ and reported under each lane relative to the value obtained in the siCON sample. Panel B: mRNA levels of APOBEC3C and PHAX after siRNA mediated knockdown compared to normal endogenous levels (siCONTROL lane) in ZIKV infected HEK 293T cells.

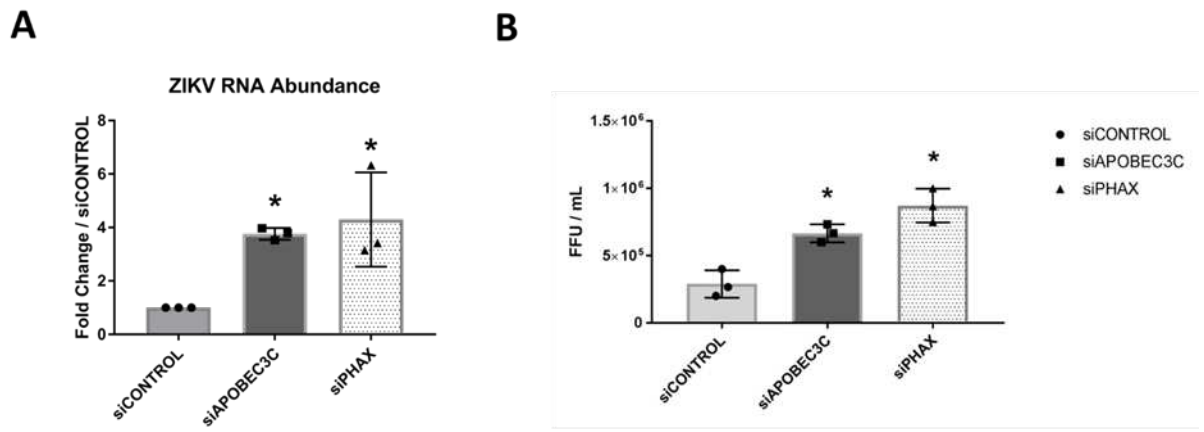

Figure 3: Knockdown experiments indicate that APOBEC3C and PHAX are negative restriction factors for ZIKV replication.

Panel A: The relative levels of ZIKV RNA in cells transfected with either a control siRNA (siCONTROL lane), a siRNA targeting APOBEC3C (siAPOBEC3C lane) or a siRNA targeting PHAX (siPHAX lane) were determined 48 hpi. The data are presented as fold change relative to the ZIKV RNA levels present in cells transfected with the control siRNA. Panel B: Focus forming assays using Vero cells infected with viral supernatant from the siRNA knockdown samples. The average number of foci per mL from three independent infections is shown. All data are the result of three independent biological experiments. * = $p<0.05$ as determined by a Students t-test.

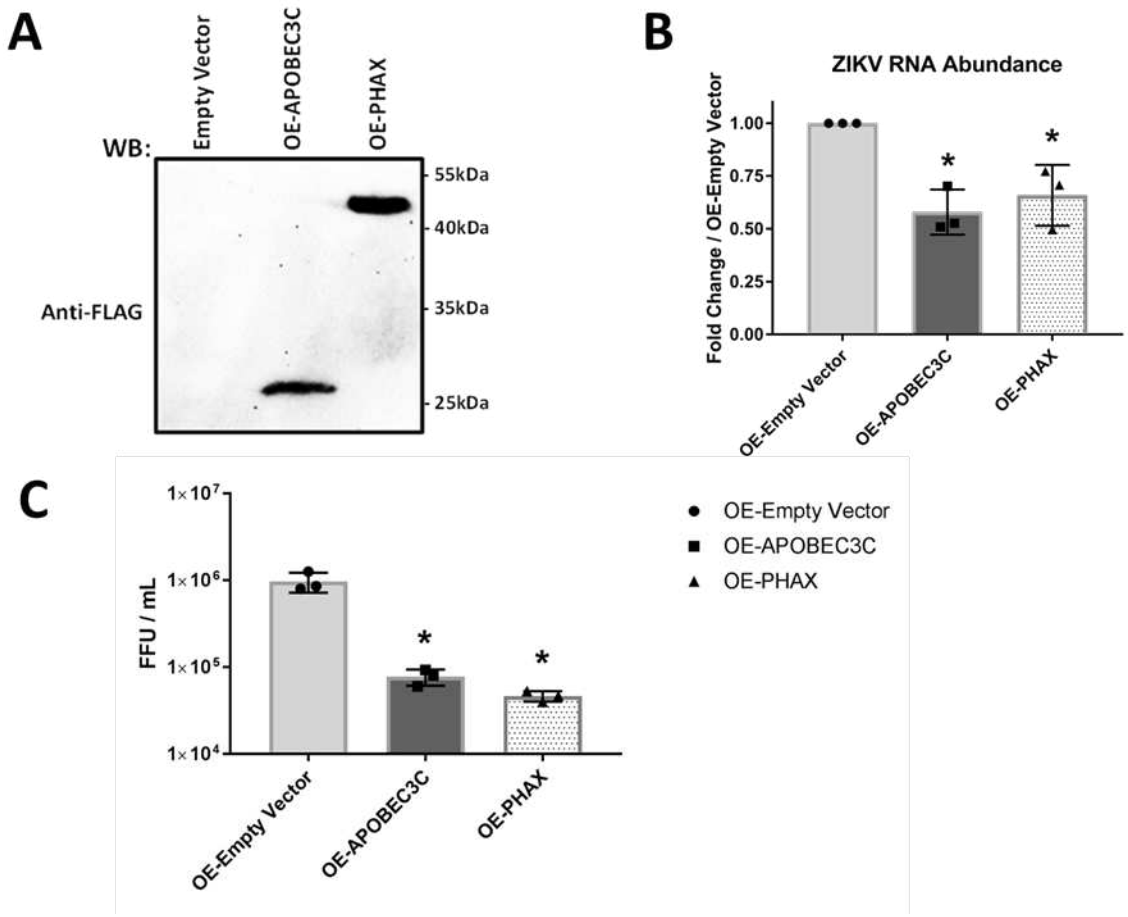

Figure 4: Exogenous expression of FLAG-tagged APOBEC3C and PHAX downregulate ZIKV replication and progeny virus production

Panel A: N-terminal FLAG-tagged versions of APOBEC3C and PHAX were constructed using expression vectors and transfected into HEK 293T cells. The levels of the indicated proteins were determined by western blot. Panel B: The relative levels of ZIKV RNA in cells transfected with either empty vector, FLAG-APOBEC3C or FLAG-PHAX expression plasmids were determined 48 hpi. The data are presented as fold change relative to the ZIKV levels present in cells transfected with the empty vector. Panel C: Focus forming assay using Vero cells infected with viral supernatant from the FLAG-tagged vector samples noted above. The average number of foci per mL from three independent infections is shown. All data are the result of three independent biological experiments. * = $p<0.05$ as determined by a Students t-test.

ZIKV infection results in dysregulation of canonical nuclear splicing patterns

Since sfRNA is sequestering two major cellular RNA splicing factors, we hypothesized that patterns of nuclear mRNA splicing may be significantly altered during ZIKV infection. SF3B1, a splicing factor that interacts strongly with sfRNA (Fig. 1C), modulates splicing for a known number of direct targets, including SRSF7, a gene that encodes a member of the SR proteins involved in splicing (Darman et al., 2015). Based on published results showing that SF3B1 knock down had dramatic effects on the splicing of the SRSF7 pre-mRNA (Darman et al., 2015), we chose to evaluate splicing of exons 2-8 of SRSF7 in HEK 293T cells during ZIKV infection (Fig. 5A). Uninfected HEK 293T cells displayed canonical transcripts where exons 2-8 are consecutively joined together as previously reported (Fig. 5B). In comparison, 48 hours post infection with ZIKV (when a substantial amount of sfRNA has accumulated within the cell), two aberrantly spliced SRSF7 mRNA transcripts were detected (Fig. 5B). Sequencing of two of these aberrantly spliced transcripts indicated that their formation resulted from the use of cryptic 5' and 3' splice sites. As diagrammed in Fig. 5C, aberrantly spliced product #1 contained a truncated exon 3 and retained a portion of intron sequence attached to exon 4. Aberrantly spliced product #2 lacked exon 3 completely and retained a portion of intron sequence attached to exon 4. Low amounts of a third aberrantly spliced product that contained exons 3-4, exon 6, and exon 8, while skipping exons 5 & 6 entirely was also obtained, which interestingly was the same aberrantly spliced product reported when SF3B1 was inhibited (Wu et al., 2018). Therefore we conclude that nuclear splicing is dysregulated during ZIKV infection in a fashion that is consistent with a mechanistic contribution of sfRNA-mediated sponging of host splicing factors.

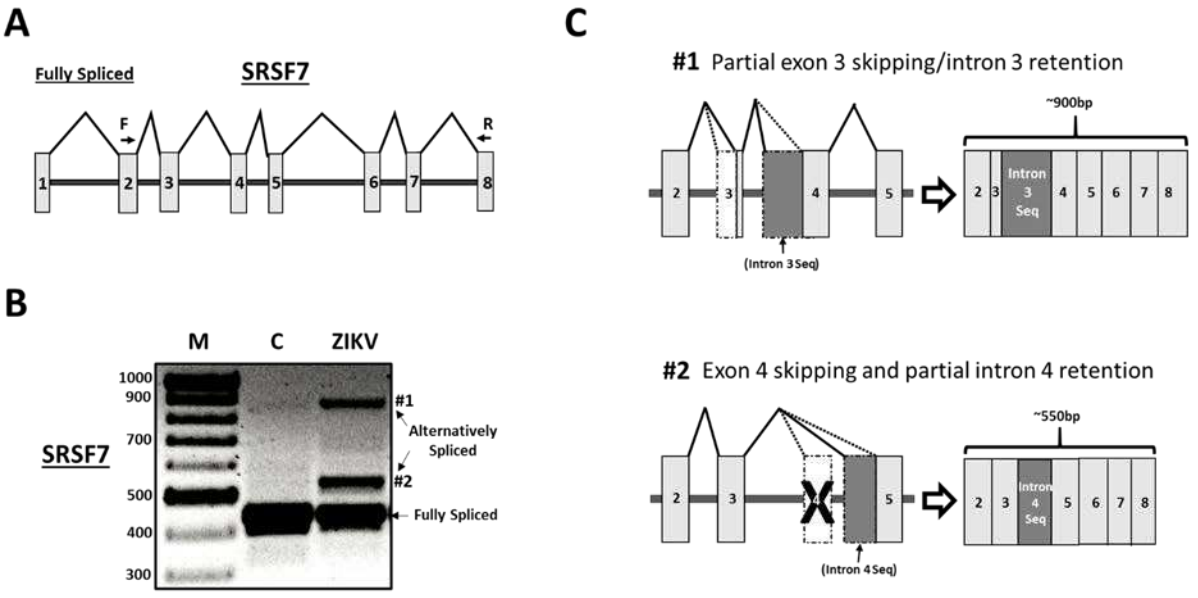

Figure 5: Splicing of a SF3B1 target gene is dysregulated during ZIKV infection
Panel A: Diagrammatic representation of exons 1-8 of SRSF7. The positions of the forward and reverse primers used to analyze splicing patterns is indicated. Panel B. Total RNA from uninfected or ZIKV infected (48 hpi) HEK 293T cells was collected and subjected to RT-PCR analysis using primers to amplify the region between exons 2-8 of the SRSF7 mRNA. Reaction products were electrophoresed on a 1% agarose gel and visualized by ethidium bromide staining. The M lanes represents a nucleic acid size marker and alternatively spliced products are indicated by the numbers at the right of the gel. Panel C: PCR products were gel purified, cloned into a pGEM-T easy vector and sequenced. The position of the resulting splice sites and exons for the indicated intermediates is indicated by the diagrams.

Investigating the mechanistic implications of APOBEC3C-sfRNA interactions in ZIKV infection

We then investigated potential changes in RNA editing due to sponging of APOBEC3C by ZIKV sfRNA through two different sequencing experiments. First, analysis of the base transversion ratios in a global RNA seq experiment comparing total RNA obtained at 12 hours post ZIKV infection and 72 hours post ZIKV infection failed to discern any difference in RNA editing (Fig. 6A). Second, sequencing of the ZIKV 3' UTR of isolates derived from wild type cells as well as cells containing overexpressed levels of APOBEC3C also failed to show any evidence of increased RNA editing (Fig. 6B). Based on these data, we conclude that APOBEC3C and ZIKV sfRNA interaction does not appear to change C->U RNA editing in infected cells. The cytidine deaminase APOBEC3C may have other, non-enzymatic impacts on ZIKV infection, such as protein-protein interaction or DNA editing that may have an effect on viral replication efficiency. A similar non-enzymatic impact of APOBEC3G on hepatitis C virus has been recently postulated (Sharma et al., 2016). Future studies will address these possibilities.

A

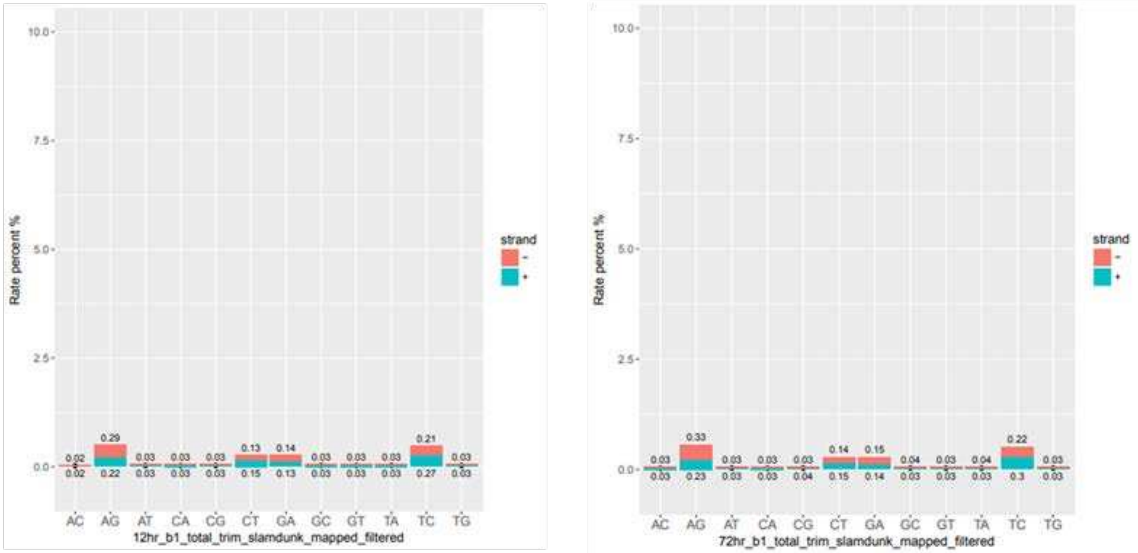

B

Number of mutations found in ZIKV 3' UTRs derived from WT vs APOBEC3C overexpressed samples		
Biological Replicate #	WT 293T Cells: # of mutations	APOBEC3C Overexpressed: # of mutations
Biological 1	0	0
Biological 2	0	0
Biological 3	0	0
Biological 4	0	0
Biological 5	0	0
Biological 6	0	0
Biological 7	0	0
Biological 8	0	0
Biological 9	0	0
Biological 10	0	0

Figure 6: Changes in G->U mutations in total RNA and ZIKV RNA do not change upon ZIKV infection or exogenous expression of APOBEC3C

Panel A: Comparison of transversion ratios at early (12 hpi) against late (72 hpi) total RNA samples from ZIKV infected cells. Panel B: Number of mutations found in ZIKV infected WT HEK293T and ZIKV infected FLAG-APOBEC3C transfected cells. The ZIKV 3' UTR was amplified from total RNA from both sets of cells, cloned into a pGEM-T easy vector and sequenced. Mutations were analyzed using Serial Cloner software.

DISCUSSION/CONCLUSION:

An estimated 2/3rds of the world's population is considered to be at risk of infection from the *Flaviviridae* family of viruses, which encompass a multitude of species including Dengue virus, Japanese encephalitis virus, West Nile virus, Tick-borne encephalitis virus and Zika virus (Pijlman et al., 2008). They are able to cause disease with an array of symptoms, from malaise that would usually be indicative of the common cold, to more serious neurological impairments such as Guillain-Barré syndrome and microcephaly (Weger-Lucarelli et al., 2017). Currently no therapeutic treatments exist for flavivirus infection. Thus, characterizing mechanisms by which flaviviruses evade the host innate-immune response and establish a productive infection is fundamentally important to the design, development and testing of novel flaviviral therapeutics.

To date, all arthropod-borne members of the *Flaviviridae* contain pseudoknot-containing three-helix junction structures in their 3' untranslated regions capable of stalling the cytoplasmic 5' - 3' exoribonuclease XRN1 (Pijlman et al., 2008; Schoenberg et al., 2012). Subsequently, the process of stalling XRN1 on these resistant RNA structures also represses its function, likely due to the slow release of the enzyme from the highly structured RNA. XRN1 repression results in a cascade of changes in RNA metabolism and RNA turnover as the cellular mRNA decay machinery is disrupted, causing changes in gene expression – in particular increasing both the abundance and stability of typically short-lived host cellular mRNAs (Moon et al., 2012). Previous work done by other members of the lab provided evidence that Zika virus sfRNA accumulation disrupts and impacts cellular mRNA decay, but I decided to broaden our perspective on the role of this non-coding viral RNA by focusing on a subset of human cellular proteins that directly interact with ZIKV sfRNA *in vivo*.

Generally speaking, ZIKV sfRNA has two known biologically relevant functions during infection: the stalling / repression of XRN1 and the binding of cellular cytoplasmic factors as a protein "sponge". By investigating sfRNAs role in protein sequestration, we uncovered that cellular factors bound to it are involved in vital host processes such as RNA decay, RNA splicing and nucleic acid editing. sfRNA-mediated sequestration of the splicing factor SF3B1 leads to the production of novel aberrantly spliced transcripts on one of the proteins key targets, SRSF7 (Fig. 5). Interestingly, SRSF7 is also an RNA splicing regulatory factor (Wu et al., 2018). Thus the aberrant splicing of SRSF7 may exponentially increase the impact of sfRNA on cellular RNA splicing. This may benefit ZIKV growth as the host cell is less able to respond to infection by altering its gene expression repertoire. The implications on cellular nucleic acid metabolism from sfRNA-APOBEC3C interactions are currently less clear. Although data clearly demonstrate a strong sfRNA-APOBEC3C interaction (Fig. 1C), the interaction does not appear to alter C->U RNA editing in infected cells (Fig. 6). Thus the APOBEC3C deaminase may instead have a role in single strand DNA editing (Timilsina et al., 2018). Alternatively, non-enzymatic functions of APOBEC3C may be involved, such as protein-protein interactions (Sharma et al., 2015; Sharma et al., 2016) that could possibly interfere with viral replication.

The targeting of XRN1 by flaviviruses appears to be a common strategy that is shared among several other families of RNA viruses. Our lab has recently demonstrated that 3' UTRs from phleboviruses and arenaviruses contain highly structured regions that are able to stall and subsequently repress XRN1 (Moon et al., 2015; Moon et al., 2012; Pijlman et al., 2008) Additionally, two segmented RNA plant viruses, Red clover necrotic mosaic virus and beet necrotic yellow vein virus, demonstrate a capacity to stall XRN1 (Iwakawa et al., 2008; Flobinus et al., 2016) due to xrRNA structures located within their genomes. Thus, exclusivity of interfacing with the cellular decay machinery to produce sub-genomic RNA cannot be given to the *Flaviviridae*. In addition, preliminary modeling studies suggests that

all XRN1 stalling structures are not created equal (J. Kieft, personal communication). The conservation of this XRN1 stalling strategy over multiple virus families from diverse evolutionary and host backgrounds suggests that it is an effective way of interfacing with the host cell. It will be interesting in the future to perform a comprehensive survey of RNA virus families to get the full picture of how RNA-based pathogens interface with this enzyme.

By targeting the cytoplasmic 5' - 3' exoribonuclease XRN1, RNA viruses disrupt a major and important pathway of RNA decay that is responsible for regulating 20-50% of gene expression within the host cell (Cheadle et al., 2005; Garcia Martinez et al., 2004; Schwanhausser et al., 2011). Disrupting this pathway can significantly dysregulate host cell gene expression during viral infection and may potentially limit the cell's ability to mount an active response against the virus. Additionally, some studies have suggested XRN1 as a possible mediator between the host transcriptional machinery and RNA decay machinery to properly modulate cellular gene expression (Haimovich et al., 2013; Sun et al., 2013). Briefly, XRN1 may play a major role in 'transcriptional buffering' which promotes homeostasis of gene expression when changes occur in either the rate of synthesis or decay of a transcript. Thus, the targeting and repression of XRN1 by RNA viruses could disrupt two distinct but linked biological processes – transcription and decay. Since RNA viruses replicate in the cytoplasm, XRN1 is highly accessible to the virus since it is a cytoplasmic enzyme. Thus by targeting XRN1, the virus does not need to facilitate RNA and protein transport into the nucleus to disrupt cellular transcription (Raices et al., 2017).

Disruption of the cellular RNA decay pathway has broad effects on the dynamics of the major RNA decay pathway in the cell. Flavivirus-mediated XRN1 repression shuts down upstream functions of the decay pathway (Moon et al., 2012; Moon et al., 2015), including deadenylation and decapping, in

addition to exonucleolytic decay. Thus when the enzyme is repressed, translatable capped and polyadenylated mRNAs, rather than deadenylated and decapped decay fragments, accumulate in the cell. How repressing XRN1 affects upstream decay processes is unclear, but our sfRNA pulldown/mass spectrometry data does provide a potential major clue. The accumulated sfRNAs during infection serve as a sponge for numerous cellular RNA binding proteins (Sessions et al., 2013) including two critically important cellular RNA decay factors, DDX6 and EDC3. Thus the sequestration of these proteins involved in decapping and coordination of translation and mRNA decay sheds insight into why upstream aspects of disruptions in RNA decay are compromised in flavivirus infections.

A key implication of the data provided in this thesis is that sfRNA-mediated sponging of other cellular factors may play a multi-faceted role in disrupting RNA biological processes in the infected cell. Accurate, efficient RNA splicing is critical for maintaining transcriptome integrity (DeMaio et al., 2016), with approximately 94% of human genes being alternatively spliced (Wang et al., 2008). A recent genome wide transcriptome analysis examining DENV-infected HEK293T cells revealed an array of cellular mRNAs which were mis-spliced. Interestingly, there was a significant increase in intron retention among these transcripts. As seen in Fig. 5, we also observed intron retention as a major impact of ZIKV infection on splicing. In addition to sfRNA-mediated sequestration of splicing factors, the DENV non-structural protein 5 (NS5) has also been shown to specifically interact with proteins of the U5 small nuclear ribonucleoprotein particle (DeMaio et al., 2016). This interaction was also implicated in reducing splicing efficiency. Mechanistic studies have indicated that binding of NS5 to the spliceosome reduces overall efficiency of pre-mRNA processing independent of NS5 enzymatic activities (DeMaio et al., 2016). Flaviviruses may use a combinatorial approach to target splicing for dysregulation during infection.

A separate transcriptome wide analysis of ZIKV infected human neural progenitor cells (hNPC) looked for virally induced aberrant splicing events in cellular RNAs (Hu et al., 2017). Interestingly, ZIKV infection induces significant changes in isoform expression, lncRNA expression, and a host of other alternative splicing events compared to mock infected cells. ZIKV-mediated RNA mis-splicing events in hNPCs appear overall to be similar to those observed in DENV interactions, suggesting that dysregulation of RNA splicing is a general strategy employed by flaviviruses, where it could prove to play a critical pro-viral role in ZIKV mediated pathogenesis. Therefore, it is intriguing to pin down the precise mechanism(s) by which this occurs during infection.

SF3B1 and PHAX proteins were found to be in complex with ZIKV and DENV sfRNAs and are both attractive cellular protein targets for cytoplasmic flaviviruses due to the fact that they shuttle between the nucleus and cytoplasm for proper function. PHAX is a cellular RNA splicing factor required for nuclear export of small nuclear RNAs (snRNAs) (Mourao et al., 2010). PHAX directly binds the snRNA in the nucleus, and with the addition of 4 other protein factors is able to form the pre-export complex (Mourao et al., 2010). Nuclear phosphorylation of PHAX is required for U snRNA export complex assembly and export into the cytoplasm. Once in the cytoplasm, PHAX dephosphorylation occurs which causes complex disassembly, and PHAX is then recycled back into the nucleus via the importin alpha/beta heterodimeric import receptor (Mourao et al., 2010). Thus, we hypothesize that sequestration of cytoplasmic PHAX by sfRNA likely interferes with cyclic nuclear shuttling of PHAX, subsequently inhibiting the protein's ability to drive the nuclear export of U snRNAs. In addition, PHAX is involved in the intranuclear transport of snoRNAs to dense regions of mRNA processing activity (Mourao et al., 2010), Cajal bodies. Thus PHAX cytoplasmic sequestration could also limit the proteins ability to transport snoRNAs appropriately, altering the regulated RNA processing occurring in Cajal bodies. These hypotheses can be tested in the future by immunofluorescence and cellular fraction studies.

SF3B1 is a cellular RNA splicing factor and a part of the U2 snRNP complex required for the major initial step of branchpoint recognition in mRNA splicing. SF3B1 has been categorized as a splicing factor, yet recent evidence suggests that it could also play a role in regulating transcription, chromatin modification and may even guide nascent transcripts to co-transcriptional splice sites (Kfir et al., 2015; Girard et al., 2012). Recently, researchers have begun to develop small designer molecules which aim to inhibit the function of this splicing protein and function as tumor-specific anticancer agents. However, conflicting reports regarding the efficacy of these agents have been reported. Interestingly, after statistical analysis of SF3B1 inhibition, the primary effect observed by one group was intron retention among cellular RNAs (Yoshimoto et al., 2017). On the other hand, another group found SF3B1 inhibition leads to a considerable amount of exon skipping in spliced transcripts (Wu et al., 2017). Thus the effects of SF3B1 inhibition are still not well understood, but the results of our study imply that both intron inclusion and exon skipping may result from sfRNA-mediated sequestration of SF3B1 during a ZIKV infection.

The AID/APOBEC family of enzymes catalyze C-to-U deamination on single stranded DNA or RNA. The APOBEC family of proteins are evolutionarily conserved and share the catalytic backbone of the zinc-dependent deaminase family. APOBEC1 has demonstrated DNA editing activity in mammalian cells, but it has also been shown that these effects can occur on herpesvirus and hepatitis viral DNA genomes (Gee et al., 2011; Gonzalez et al., 2009). DNA/RNA editing is a prevalent epitranscriptomic modification which has a wide range of effects on host cells and viruses that are still not fully understood. In HIV infected cells, human APOBEC3G serves a defensive role where the protein induces G to A hypermutations in the HIV-1 genome (Sheehy et al., 2002). Previously, others have reported that APOBEC3G serves as a cellular restriction factor against hepatitis C virus (HCV) (Peng et al., 2011).

Interestingly, APOBEC3G directly interfaces with the NS3 protein of HCV resulting in decreased NS3 helicase activity (Zhu et al., 2015). Thus there is precedence in the literature for APOBEC-mediated replication restriction of RNA viruses, yet questions remain with regard to how APOBEC3C is actually restricting flavivirus infection. APOBEC3C may restrict ZIKV replication through other methods, perhaps through various protein-protein and/or protein-RNA interactions. Additionally, it us unknown whether APOBEC3C is packaged into ZIKV virions as APOBEC3G has been shown to be packaged with HIV virions. Experiments to assess this using purified virions have been planned for future studies.

A closer analysis of the knockdown/overexpression data for APOBEC3C and PHAX on ZIKV replication in Figures 3 and 4 may reveal two functional implications. First, an approximately 2X overexpression of either APOBEC3C or PHAX led to a ten-fold reduction in focus forming units. This lack of stoichiometry between the relative levels of protein expression and viral replication suggests that the factors are interfering with an amplifiable aspect of the infection such as a viral RNA polymerase. Second, the knockdown of these cellular factors only had a 2-4 effect on viral RNA or virion production. This effect may be lower than overexpression due to the idea that the sfRNA being made by the virus is already sequestering/inhibiting a large amount of the endogenous proteins in the infected cell. Thus reducing the overall amount of the already virally-debilitated protein would be expected to have a limited effect. Thus these data may be consistent with our model that sequestration of the proteins by sfRNA has a significant biological effect in the infected cell.

As seen in Fig. 1B, an additional 15+ RNA binding proteins were identified in our RNA-pull down and mass spectrometry experiment that have not been explored in greater depth to date. These RBPs include multiples host RNA splicing factors that could perform pivotal roles in mediating the significant degree of aberrant splicing induced by flavivirus infections in human cells. RTCB, a potentially important

protein identified in our experiments, is a tRNA splicing factor that is the catalytic component of the tRNA-splicing ligase complex. RTCB functions to directly join two spliced tRNA-halves into a single, mature tRNA molecule. Evidence suggests RTCB also possesses RNA ligase activity with the ability to target a broad range RNA species and has been specifically shown to ligate XBP1 fragments during endoplasmic reticulum stress (Lu et al., 2014; Nandy et al., 2017).

In summary, this thesis has revealed several key aspects of flavivirus biology, yet it is very clear that detailed molecular mechanisms responsible for flaviviral mediated cytopathology and pathogenesis remain to be pursued in the future. Our work clearly highlights the importance of the highly abundant virally-derived sfRNA transcripts and their role in cytopathology and pathogenesis, and overall the impact of sfRNA-mediated sequestration of proteins and their subsequent repression of their normal cellular functions.

REFERENCES:

Akiyama BM, Laurence HM, Massey AR, Costantino DA, Xie X, Yang Y, Shi PY, Nix JC, Beckham JD, Kieft JS. Zika virus produces noncoding RNAs using a multi-pseudoknot structure that confounds a cellular exonuclease. Science 2016; 354:1148–52.

Barnhart MD, Moon SL, Emch AW, Wilusz CJ, Wilusz J. Changes in cellular mRNA stability, splicing, and polyadenylation through HuR protein sequestration by a cytoplasmic RNA virus. Cell Rep 2013; 5:909–17.

Bidet K, Dadlani D, Garcia-Blanco MA. Correction: G3BP1, G3BP2 and CAPRIN1 Are Required for Translation of Interferon Stimulated mRNAs and Are Targeted by a Dengue Virus Non-coding RNA. PLoS Pathog. 2017; 13:e1006295

Chapman EG, Moon SL, Wilusz J, Kieft JS. RNA structures that resist degradation by Xrn1 produce a pathogenic Dengue virus RNA. Elife 2014; 3:e01892.

Cheadle C, Fan J, Cho-Chung YS, Werner T, Ray J, Do L, Gorospe M, Becker KG. Control of gene expression during T cell activation: alternate regulation of mRNA transcription and mRNA stability. BMC Genomics 2005; 6: 75.

Darman RB, Seiler M, Agrawal AA, Lim KH, Peng S, Aird D, Bailey SL, Bhavsar EB, Chan B, Colla S, et al. Cancer-Associated SF3B1 Hotspot Mutations Induce Cryptic 3' Splice Site Selection through Use of a Different Branch Point. Cell Rep 2015; 13:1033–45.

De Maio FA, Risso G, Iglesias NG, Shah P, Pozzi B, Gebhard LG, Mammi P, Mancini E, Yanovsky MJ, Andino R, et al. The Dengue Virus NS5 Protein Intrudes in the Cellular Spliceosome and Modulates Splicing. ed. T.C. Pierson. PLoS Pathog 2016; 12: e1005841.

Flobinus A, Hleibieh K, Klein E, Ratti C, Bouzoubaa S, Gilmer D. A Viral Noncoding RNA Complements a Weakened Viral RNA Silencing Suppressor and Promotes Efficient Systemic Host Infection. Viruses. 2016; 8: 272.

Ford LP, Watson J, Keene JD, Wilusz J. ELAV proteins stabilize deadenylated intermediates in a novel in vitro mRNA deadenylation/degradation system. Genes Dev 1999; 13:188–201.

Funk A, Truong K, Nagasaki T, Torres S, Floden N, Balmori Melian E, Edmonds J, Dong H, Shi P-Y, Khromykh AA. RNA structures required for production of subgenomic flavivirus RNA. J Virol 2010; 84:11407–17.

García-Martínez J, Aranda A, Pérez-Ortín JE. Genomic run-on evaluates transcription rates for all yeast genes and identifies gene regulatory mechanisms. Mol Cell 2004; 15: 303–313.

Gee P, Ando Y, Kitayama H, Yamamoto SP, Kanemura Y, Ebina H, Kawaguchi Y, Koyanagi Y. APOBEC1-mediated editing and attenuation of herpes simplex virus 1 DNA indicate that neurons have an antiviral role during herpes simplex encephalitis. J Virol. 2011; 85: 9726–9736.

Girard C, Will CL, Peng J, Makarov EM, Kastner B, Lemm I, Urlaub H, Hartmuth K, Lührmann R. Post-transcriptional spliceosomes are retained in nuclear speckles until splicing completion. Nat Commun. 2012; 3: 994.

Gonzalez MC, Suspène R, Henry M, Guétard D, Wain-Hobson S, Vartanian J-P. Human APOBEC1 cytidine deaminase edits HBV DNA. Retrovirology. 2009; 6: 96.

Haimovich G, Medina DA, Causse SZ, Garber M, Millán-Zambrano G, Barkai O, Chávez S, Pérez-Ortín JE, Darzacq X, Choder M. Gene expression is circular: factors for mRNA degradation also foster mRNA synthesis. Cell. 2013; 153: 1000–1011.

Hu B, Huo Y, Yang L, Chen G, Luo M, Yang J, Zhou J. ZIKV infection effects changes in gene splicing, isoform composition and lncRNA expression in human neural progenitor cells. Virol J 2017; 14:217.

Iwakawa H-O, Mizumoto H, Nagano H, Imoto Y, Takigawa K, Sarawaneeyaruk S, Kaido M, Mise K, Okuno T. A viral noncoding RNA generated by cis-element-mediated protection against 5“->3” RNA decay represses both cap-independent and cap-dependent translation. J Virol. 2008; 82: 10162–10174.

Kfir N, Lev-Maor G, Glaich O, Alajem A, Datta A, Sze SK, Meshorer E, Ast G. SF3B1 association with chromatin determines splicing outcomes. Cell Rep. 2015; 11: 618–629.

Kung C-P, Maggi LB, Weber JD. The Role of RNA Editing in Cancer Development and Metabolic Disorders. Front Endocrinol (Lausanne) 2018; 9:762.

Lerner T, Papavasiliou FN, Pecori R. RNA Editors, Cofactors, and mRNA Targets: An Overview of the C-to-U RNA Editing Machinery and Its Implication in Human Disease. Genes (Basel) 2018; 10:13.

Liao K-C, Chuo V, Ng WC, Neo SP, Pompon J, Gunaratne J, Ooi EE, Garcia-Blanco MA. Identification and characterization of host proteins bound to dengue virus 3' UTR reveal an antiviral role for quaking proteins. RNA. 2018; 24: 803–814.

Lu Y, Liang F-X, Wang X. A synthetic biology approach identifies the mammalian UPR RNA ligase RtcB. Mol Cell. 2014; 55: 758–770.

Mangeat B, Turelli P, Caron G, Friedli M, Perrin L, Trono D. Broad antiretroviral defense by human APOBEC3G through lethal editing of nascent reverse transcripts. Nature. 2003; 424: 99–103.

Moon SL, Anderson JR, Kumagai Y, Wilusz CJ, Akira S, Khromykh AA, Wilusz J. A noncoding RNA produced by arthropod-borne flaviviruses inhibits the cellular exoribonuclease XRN1 and alters host mRNA stability. RNA 2012; 18:2029–40.

Moon SL, Wilusz J. Cytoplasmic viruses: rage against the (cellular RNA decay) machine. PLoS Pathog 2013; 9:e1003762.

Moon SL, Blackinton JG, Anderson JR, Dozier MK, Dodd BJT, Keene JD, Wilusz CJ, Bradrick SS, Wilusz J. XRN1 stalling in the 5' UTR of Hepatitis C virus and Bovine Viral Diarrhea virus is associated with dysregulated host mRNA stability. PLoS Pathog. 2015a; 11:e1004708.

Moon SL, Dodd BJT, Brackney DE, Wilusz CJ, Ebel GD, Wilusz J. Flavivirus sfRNA suppresses antiviral RNA interference in cultured cells and mosquitoes and directly interacts with the RNAi machinery. Virology. 2015b; 485:322–9.

Mourão A, Varrot A, Mackereth CD, Cusack S, Sattler M. Structure and RNA recognition by the snRNA and snoRNA transport factor PHAX. RNA 2010; 16:1205–16.

Mukherjee D, Gao M, O'Connor JP, Raijmakers R, Pruijn G, Lutz CS, Wilusz J. The mammalian exosome mediates the efficient degradation of mRNAs that contain AU-rich elements. EMBO J 2002; 21:165–74.

Nandy A, Saenz-Méndez P, Gorman AM, Samali A, Eriksson LA. Homology model of the human tRNA splicing ligase RtcB. Proteins. 2017; 85: 1983–1993.

Peng Z-G, Zhao Z-Y, Li Y-P, Wang Y-P, Hao L-H, Fan B, Li Y-H, Wang Y-M, Shan Y-Q, Han Y-X, et al. Host apolipoprotein B messenger RNA-editing enzyme catalytic polypeptide-like 3G is an innate defensive factor and drug target against hepatitis C virus. Hepatology. 2011; 53: 1080–1089.

Petrova E, Gracias S, Beauclair G, Tangy F, Jouvenet N. Uncovering Flavivirus Host Dependency Factors through a Genome-Wide Gain-of-Function Screen. Viruses 2019; 11:68.

Pijlman GP, Funk A, Kondratieva N, Leung J, Torres S, van der Aa L, Liu WJ, Palmenberg AC, Shi P-Y, Hall RA, et al. A highly structured, nuclease-resistant, noncoding RNA produced by flaviviruses is required for pathogenicity. Cell Host Microbe. 2008; 4:579–91.

Raices M, D'Angelo MA. Nuclear pore complexes and regulation of gene expression. Curr Opin Cell Biol. 2017; 46: 26–32.

Schwanhäusser B, Busse D, Li N, Dittmar G, Schuchhardt J, Wolf J, Chen W, Selbach M. Global quantification of mammalian gene expression control. Nature. 2011; 473: 337–342.

Schoenberg DR, Maquat LE. Regulation of cytoplasmic mRNA decay. Nat Rev Genet 2012; 13:246–59.

Sessions OM, Tan Y, Goh KC, Liu Y, Tan P, Rozen S, Ooi EE. Host cell transcriptome profile during wild-type and attenuated dengue virus infection. ed. E. Harris. PLoS Negl Trop Dis. 2013; 7: e2107.

Sharma S, Patnaik SK, Taggart RT, Kannisto ED, Enriquez SM, Gollnick P, Baysal BE. APOBEC3A cytidine deaminase induces RNA editing in monocytes and macrophages. Nat Commun 2015; 6:6881.

Sharma S, Patnaik SK, Taggart RT, Baysal BE. The double-domain cytidine deaminase APOBEC3G is a cellular site-specific RNA editing enzyme. Sci Rep 2016; 6:39100.

Sheehy AM, Gaddis NC, Choi JD, Malim MH. Isolation of a human gene that inhibits HIV-1 infection and is suppressed by the viral Vif protein. Nature. 2002; 418: 646–650.

Silva PAGC, Pereira CF, Dalebout TJ, Spaan WJM, Bredenbeek PJ. An RNA pseudoknot is required for production of yellow fever virus subgenomic RNA by the host nuclease XRN1. J Virol 2010; 84:11395–406.

Slonchak A, Khromykh AA. Subgenomic flaviviral RNAs: What do we know after the first decade of research. Antiviral Res 2018; 159:13–25.

Sokoloski KJ, Wilusz J, Wilusz CJ. The preparation and applications of cytoplasmic extracts from mammalian cells for studying aspects of mRNA decay. Meth Enzymol. 2008; 448:139–63.

Steckelberg A-L, Akiyama BM, Costantino DA, Sit TL, Nix JC, Kieft JS. A folded viral noncoding RNA blocks host cell exoribonucleases through a conformationally dynamic RNA structure. Proc Natl Acad Sci USA. 2018; 115:6404–9.

Sun M, Schwalb B, Pirkl N, Maier KC, Schenk A, Failmezger H, Tresch A, Cramer P. Global analysis of eukaryotic mRNA degradation reveals Xrn1-dependent buffering of transcript levels. Mol Cell. 2013; 52: 52–62.

Timilsina U, Ghimire D, Sharma S, Gaur R. Role of APOBEC3 proteins in proteasome inhibitor-mediated reactivation of latent HIV-1 viruses. J Gen Virol 2018; 4:432.

Weger-Lucarelli J, Duggal NK, Brault AC, Geiss BJ, Ebel GD. Rescue and Characterization of Recombinant Virus from a New World Zika Virus Infectious Clone. J Vis Exp 2017; :e55857.

Wang ET, Sandberg R, Luo S, Khrebtukova I, Zhang L, Mayr C, Kingsmore SF, Schroth GP, Burge CB. Alternative isoform regulation in human tissue transcriptomes. Nature. 2008; 456: 470–476.

Wu G, Fan L, Edmonson MN, Shaw T, Boggs K, Easton J, Rusch MC, Webb TR, Zhang J, Potter PM. Inhibition of SF3B1 by molecules targeting the spliceosome results in massive aberrant exon skipping. RNA 2018; 24:1056–66.

Yoshimoto R, Kaida D, Furuno M, Burroughs AM, Noma S, Suzuki H, Kawamura Y, Hayashizaki Y, Mayeda A, Yoshida M. 2017. Global analysis of pre-mRNA subcellular localization following splicing inhibition by spliceostatin A. RNA 23: 47–57.

Zhu Y-P, Peng Z-G, Wu Z-Y, Li J-R, Huang M-H, Si S-Y, Jiang J-D. Host APOBEC3G protein inhibits HCV replication through direct binding at NS3. ed. E. Villa. PLoS ONE. 2015; 10: e0121608.